Chinese Chemical Letters 31 (2020) 64–66

Contents lists available at ScienceDirect

Chinese Chemical Letters

journal homepage: www.elsevier.com/locate/cclet

Communication

Synthesis and application of a novel 9,9-diethyl-1,2-diaryl-1,9-dihydrofluoreno[2,3-*d*]imidazole for blue organic light emitting diode

Xueying Wang[a], Zhangcheng Liao[a,b], Tianqi Wang[a], Haixia Lin[a], Zixing Wang[b,*], Yongmei Cui[a,*]

[a] *Department of Chemistry, College of Sciences, Shanghai University, Shanghai 200444, China*
[b] *Key Laboratory of Advanced Display and System Applications, Ministry of Education, Shanghai University, Shanghai 200072, China*

ARTICLE INFO

Article history:
Received 29 March 2019
Received in revised form 22 May 2019
Accepted 23 May 2019
Available online 23 May 2019

Keywords:
Fluorene
Imidazole
Photoluminescence
Electroluminescence

ABSTRACT

Two novel 2-(4-(9,9-disubstitued-9*H*-fluoren-2-yl)phenyl)-9,9-diethyl-1-phenyl-1,9-dihydrofluoreno-[2,3-*d*]imidazole derivatives **2a** and **2b** were synthesized and characterized. Their photophysical and electrochemical properties, thermal stability property, and electroluminescence (EL) performance of **2b** were investigated. The fabricated device based on **2b** doping into 4,4′-*N*,*N*'-dicarbazole-biphenyl (5%) as an emitter present a maximum brightness of 1272 cd/m^2 at 4 V with the CIE coordinate of (0.1590, 0.0465).

Since efficient organic light-emitting diodes (OLEDs) were reported by Tang and Van Slyke [1], OLEDs have attracted more and more attention due to their potential applications in flat panel displays [2–6]. Although numerous classes of light emitting organic semiconductors have been designed and developed, deep-blue emitters with high efficiency are still scarce and efforts are still continuing in order to find efficient pure blue light emitting materials for OLEDs [7–12]. Blue light emitting materials play important roles in energy-efficient solid-state lighting and smart display devices. Energy-efficient OLEDs are considered one of the most competitive candidates for next generation smart displays and particularly for future energy-saving lighting sources [13,14]. Recently, much effort has been devoted to attempts to generate white OLEDs comprising both fluorescent and phosphorescent materials [15,16]. Efficient blue-emitting materials are also one of the important key elements for fabricating white OLED devices [17–21]. Among various blue light-emitting materials, fluorene-based polymers or oligomers have attracted extensive interest due to their excellent blue light-emitting ability, easily processing, good thermal and electrochemical stabilities [22–28]. Although many blue light-emitting materials based on fluorenes have been reported, the EL efficiencies of these deep-blue OLEDs (Commission Internationale de L'Eclairage (CIE) y coordinate value < 0.15 along with an $(x+y)$ value < 0.30) are rather poor compared to those of sky-blue OLEDs (CIE coordinates of $x = 0.15$ and $y > 0.15$) [7]. Therefore, the search for new efficient deep-blue fluorescent materials with high performance remains a major challenge.

In the search of new luminophores for use in light-emitting materials, we have successfully synthesized a series of new fluorene derivatives based on 3,9-dihydro-9,9-dioctylfluoreno[3,2-*d*]imidazole (DOFI), 10,10-dioctyl-3,6-dihydrofluoreno[2,3-*d*:6,7-*d*']diimidazoles (DOFDIs) [29,30] and 9,9-diethyl-1,2-diaryl-1,9-dihydrofluoreno[2,3-*d*]imidazoles [30], which emit blue fluorescence and have acceptable fluorescence quantum yields. In this letter, we report the synthesis and blue light-emitting properties of two new 9,9-diethyl-1,2-diaryl-1,9-dihydrofluoreno[2,3-*d*]imidazoles (**2a**, **2b**) by introducing a fluorene group into the 9,9-diethyl-1,2-diphenyl-1,9-dihydrofluoreno[2,3-*d*]imidazole (**1a**) core. The synthesis and characterization of **2a-b**, including their photophysical and electrochemical properties, thermal stability property, and electroluminescence (EL) performance of **2b** were well performed. Compounds **2a-b** were synthesized by palladium-catalyzed Suzuki cross-coupling reaction of 2-(4-bromophenyl)-9,9-diethyl-1-phenyl-1,9-dihydrofluoreno[2,3-d]imidazole (**1b**) [31] and fluorene boric acid as outlined in Scheme 1. Fig. 1 and Table 1 display the absorption and photoluminescence (PL) spectra upon excitation at each excitation wavelength (λ_{ex}) at room temperature in CH_2Cl_2 and DMSO solutions. As shown in Fig. 1, both compounds **2a-b** display almost the same absorption characteristics, showing two peaks at *ca.* 280, 351 nm and 289, 352 nm, respectively, which can be attributed to different π–π^* transitions. The UV–vis absorption maxima of compounds **2a-b**

---

* Corresponding authors.
E-mail addresses: zxwang78@shu.edu.cn (Z. Wang), ymcui@shu.edu.cn (Y. Cui).

https://doi.org/10.1016/j.cclet.2019.05.044

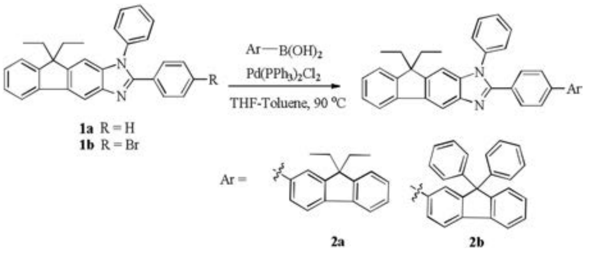

Scheme 1. The synthetic route of the compounds.

were red-shifted by *ca.* 14 nm relative to that of **1a**, due to the elongation of conjugation length. It was observed that the absorption spectra changed very little with the increase of solvent polarity although there was a tendency of a longer λ_{max} in DMSO, indicating that there was no charge transfer in the ground state. With the introduction of fluorene group, the peaks of the fluorescent spectra shift from the near UV region to the blue region. In CH_2Cl_2 solution, compound **2a** showed emission peak at 428 nm (Fig. 1a) and the fluorescence quantum yield is 0.86, which is higher than that of quinine sulfate (Φ_{FL} = 0.55). It is interesting to note that compound **2b** shows strong blue fluorescence-emitting ability with Φ_{FL} value of 0.55, with PL emission peak at 430 nm slightly red-shifted by 2 nm relative to **2a**. Moreover, both compounds were slightly red-shifted in DMSO relative to those in CH_2Cl_2. Comparing the absorption and fluorescence spectra of **2a**, **2b** and **1a** indicates that absorption and fluorescence are determined by the whole conjugation system and substitutions at the C-9 position of the fluorene have little influence on the optical properties of the molecule.

The HOMO and LUMO of **2a** and **b** were determined by the cyclic voltammetrical analysis and UV–vis absorption edge. The measured HOMO levels for **2a** and **2b** are −5.56 and −5.53 and their LUMO levels are −2.38 and −2.42, respectively. Therefore, substitutions at the C9 position have little impact on their frontier energy levels. Apparently, these two compounds exhibit wide bandgaps and this is suitable for their use as blue emitters. To provide a better insight into the geometries and electron-state-density distributions of the fluorophores, DFT calculation at B3LYP/6-31 G(d) level was performed, as provided in Fig. 2. In the optimized ground state geometry, **2a** and **2b** show twisted structures with a dihedral angle around 15° between the phenyl spacer and plane of fluoreno[2,3-d]imidazole. The electron cloud distribution of the two compounds is almost similar. The HOMO state density of the two fluorophores mainly distributes on the fluorenoimidazole skeleton and the bridging phenyl ring, spreading on the phenyl ring of the terminal fluorene. On the other hand,

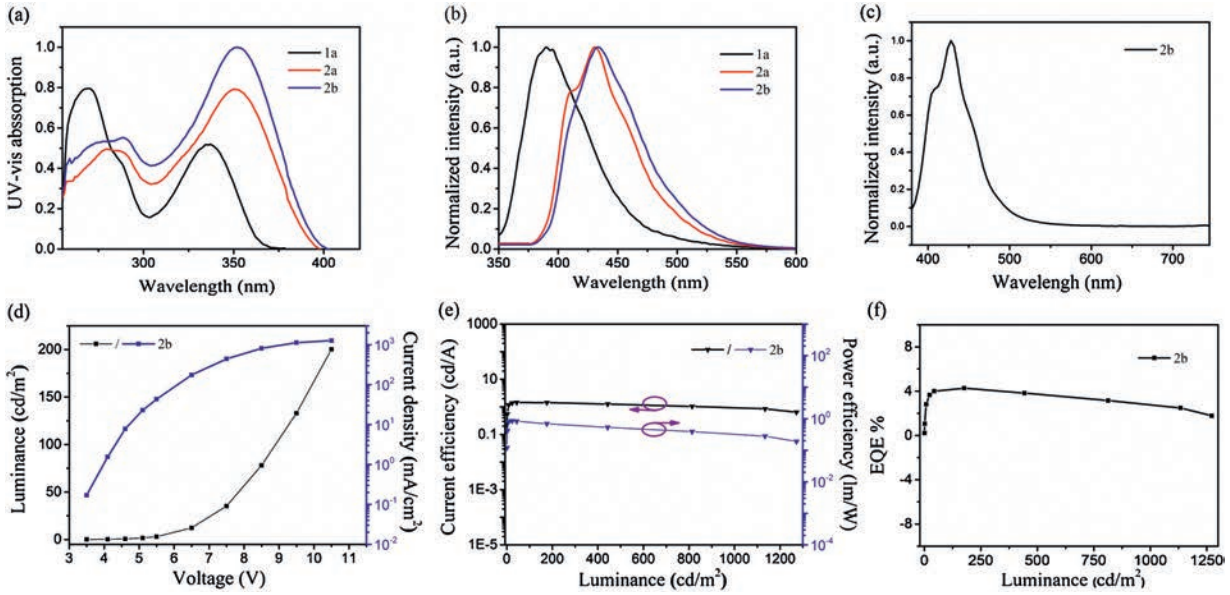

Fig. 1. UV–vis spectra (a, 5 × 10⁻⁵ mol/L) and fluorescence spectra (b, 5 × 10⁻⁷ mol/L) of compounds in CH_2Cl_2; (c) EL spectrum of compound **2b**; (d) The J-V-L characteristics; (e) The η_c-L–η_p characteristics; (f) the EQE%-L.

Table 1
The absorption characteristics and optical properties of the three compounds.

Compound	λ_{abs} (nm)[a]		λ_{ex} (nm)[b]		λ_{em} (nm)[c]		Φ_{FL}[d]	HOMO[e]	LUMO[f]	E_{ox}[g]	E_g[h]
	CH_2Cl_2	DMSO	CH_2Cl_2	DMSO	CH_2Cl_2	DMSO					
1a	269,337	269,338	344	347	379	382	0.84	−5.52	−2.17	0.92	3.35
2a	280,351	282,353	360	362	428	428	0.86	−5.56	−2.38	0.96	3.18
2b	289,352	291,355	360	363	430	432	0.88	−5.53	−2.42	0.93	3.11

[a] UV-vis absorption wavelength in CH_2Cl_2 or in DMSO at room temperature.

[b] Excitation wavelength in CH_2Cl_2 or in DMSO at room temperature.

[c] Fluorescence wavelength in CH_2Cl_2 or in DMSO at room temperature.

[d] Fluorescence quantum yields, measured in CH_2Cl_2 solution using a 0.2 mol/L H_2SO_4 solution of quinine sulfate (Φ_{FL} = 0.55) as a reference.

[e] HOMO energy levels derived from the oxidation potential using HOMO = - E_{ox} - 4.60.

[f] LUMO energy levels were deduced using the formula LUMO = HOMO + E_g.

[g] E_{ox}, the onset of oxidation potentials were measured with cyclic voltammetry system.

[h] E_g = 1240/UV(onset). UVs (onset) were estimated from the onset of the absorption spectra.

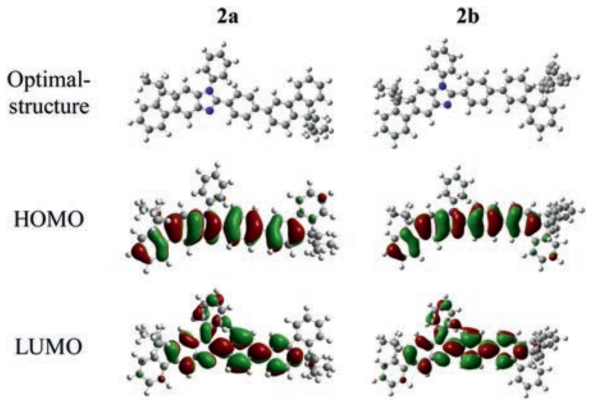

Fig. 2. Optimal structures and the distributions of the frontier levels (HOMO, LUMO) for **2a** and **b**.

the LUMO state electron density mainly locates on the benzoimidazole ring, *N*-1 phenyl group and the interconnected phenyl ring with a minor contribution from the phenyl ring of the fluorene unit. The calculated HOMO levels were −5.19, −5.42 eV, while the LUMO levels were −1.45, −1.76 eV for **2a** and **2b**, respectively. The predicted HOMO and LUMO energies show good agreement with the experimental results although there are some discrepancies.

Compound **2b** exhibited good thermal stability with a high decomposition temperature (T_d: corresponding to 5 wt% mass loss) of 350 °C and a high glass transition temperature (T_g) of 490 °C, which is suffice for application in OLEDs. To explore the potential of **2b** as active ingredient, we fabricated blue fluorescence OLEDs by multi-layer vacuum deposition with the device configuration of ITO / HATCN (5 nm) / NPB (20 nm) / TCTA (10 nm) / CBP: **2b** (5%) (20 nm) / TMPYPB (40 nm) / LiQ (1 nm) / Al (80 nm), in which ITO (indium tin oxide) was used as anode, HATCN (1,4,5,8,9,11-hexaaza triphenylene-hexacarbonitrile) used as the hole injection layer (HIL), NPB (*N*,*N*′-bis-(1-naphthyl)-l)-*N*,*N*′-diphenyl-[1,1′-biphenyl]-4,4′-diamine) used as the hole blocking layer (HBL), TCTA (4,4′,4′′-tris(carbazol-9-yl)-triphenylamine) used as the exciton blocking layer (EBL), the **2b** (5% concentration) doped in the CBP (4,4′-*N*,*N*′-dicarbazole-biphenyl) host material was used as the emitting layer (EML), TmPYPB (3,3′-(5′-(3-(pyridin-3-yl)phenyl)-[1,1′:3′,1′′-terphenyl]-3,3′′-diyl)dipyridine) used as the electron transporting layer (ETL), LiQ (lithium 8-hydroxyquinolate) used as the electron injecting layer (EIL), Al was used as the cathode. The EL spectrum of this device shows blue emission maxima at around 428 nm, which was almost the same as compared to that obtained from CH_2Cl_2 solution. This doped device is located in the deep-blue region with CIE (x, y) values of (0.1590, 0.0465), exhibits a maximum luminance of 1272 cd/m^2 at 4 V, a maximum luminance efficiency of 1.45 cd/A, a maximum power efficiency of 0.85 lm/W and a maximum external quantum efficiency of 4.72%.

In summary, two 2-(4-(9,9-disubstitued-9*H*-fluoren-2-yl)phenyl)-9,9-diethyl-1-phenyl-1,9-dihydrofluoreno[2,3-*d*]imidazole derivatives **2a** and **2b** were designed and synthesized for application in doped blue OLEDs. The fabricated device based on **2b** doping into 4,4′-*N*,*N*′-dicarbazole-biphenyl (5%) as an emitter shows a good performance with maximum EL peak at 428 nm, a maximum luminance of 1272 cd/m^2 at 4 V, a maximum luminance efficiency of 1.45 cd/A, a maximum power efficiency of 0.85 lm/W and CIE coordinate (0.1590, 0.0465), approaching EBU deep blue standard [32]. Further research regarding the incorporation of these systems usable as organic light-emitting diodes will be reported in due course.

Acknowledgment

This study was supported by the National Natural Science Foundation of China (Nos. 81202402, 21272154).

References

[1] C.W. Tang, S.A. VanSlyke, Appl. Phys. Lett. 51 (1987) 913–915.
[2] Y.J. Luo, Z.Y. Lu, Y. Huang, et al., Chin. Chem. Lett. 27 (2016) 1223–1230.
[3] Z. Huang, S. Xiang, Q. Zhang, et al., J. Mater. Chem. C 6 (2018) 2379–2386.
[4] Z.H. Li, M.J. Xiong, M.S. Wong, Chin. Chem. Lett. 18 (2007) 823–826.
[5] H.X. Xu, F. Wang, K.X. Wang, et al., Dyes Pigm. 155 (2018) 84–92.
[6] C.K. Liu, Y.H. Chen, Y.J. Long, et al., Dyes Pigm. 157 (2018) 101–108.
[7] M. Zhu, C. Yang, Chem. Soc. Rev. 42 (2013) 4963–4976.
[8] P.K. Samanta, D. Kim, V. Coropceanu, et al., J. Am. Chem. Soc. 139 (2017) 4042–4051.
[9] Y. Tan, Z. Zhao, L. Shang, et al., J. Mater. Chem. C 5 (2017) 11901–11909.
[10] A. Abdurahman, A. Obolda, Q. Peng, et al., Dyes Pigm. 153 (2018) 10–17.
[11] M. Jung, J. Lee, H. Jung, et al., Dyes Pigm. 158 (2018) 42–49.
[12] T. Shan, Y. Liu, X. Tang, et al., ACS Appl. Mater. Inter. 8 (2016) 28771–28779.
[13] N. Thejokalyani, S.J. Dhoble, Renew. Sust. Energ. Rev. 32 (2014) 448–467.
[14] J. Moon, E. Kim, S.K. Park, et al., Org. Electron. 26 (2015) 273–278.
[15] L.S. Cui, Y. Liu, X.Y. Liu, et al., ACS Appl. Mater. Inter. 7 (2015) 11007–11014.
[16] J. Wan, C.J. Zheng, M.K. Fung, et al., J. Mater. Chem. 22 (2012) 4502–4510.
[17] N. Sun, Q. Wang, Y. Zhao, et al., Adv. Mater. 26 (2014) 1617–1621.
[18] Y. Sun, N.C. Giebink, H. Kanno, et al., Nature 440 (2006) 908–912.
[19] G. Schwartz, K. Fehse, M. Pfeiffer, et al., Appl. Phys. Lett. 89 (2006) 083509–083512.
[20] X. Yang, Z. Wang, S. Madakuni, et al., Adv. Mater. 20 (2008) 2405–2409.
[21] K.T. Kamtekar, A.P. Monkman, M.R. Bryce, Adv. Mater. 22 (2010) 572–582.
[22] W. Sun, N. Zhou, Y. Xiao, et al., Chem. Asian J. 12 (2017) 3069–3076.
[23] W. Sun, N. Zhou, Y. Xiao, et al., Dyes Pigm. 154 (2018) 30–37.
[24] K.T. Wong, R.T. Chen, F.C. Fang, et al., Org. Lett. 7 (2005) 1979–1982.
[25] C.G. Zhen, Z.K. Chen, Q.D. Liu, et al., Adv. Mater. 21 (2009) 2425–2429.
[26] J.H. Jou, S. Kumar, P.H. Fang, et al., J. Mater. Chem. C 3 (2015) 2182–2194.
[27] C.C. Wu, Y.T. Lin, H.H. Chiang, et al., Appl. Phys. Lett. 81 (2002) 577–579.
[28] N. Matsumoto, T. Miyazaki, M. Nishiyama, et al., J. Phys. Chem. C 113 (2009) 6261–6266.
[29] J.G. Guo, Y.M. Cui, H.X. Lin, et al., J. Photoch. Photobiol. 219 (2011) 42–49.
[30] H.F. Chen, Y.M. Cui, J.G. Guo, et al., Dyes Pigm. 94 (2012) 583–591.
[31] T.Q. Wang, S.L. Zhao, W.M. Zhang, H.X. Lin, Y.M. Cui, Monatsh. Chem. 147 (2016) 1991–1999.
[32] E.J. Lee, Y.H. Ha, Ieee Trans. Consum. Electron. 44 (1998) 10–15.